

An Architecture for Design and Analysis of High-Performance Robust Anti-Windup Compensators

Andrés Marcos, Matthew C. Turner and Ian Postlethwaite

Abstract

In this paper, a general framework for the design and analysis of robust anti-windup compensators is presented. The proposed framework combines the Weston-Postlethwaite anti-windup scheme with ideas from residual generation and robust high-performance control architectures. It is shown that the framework is well connected to the Youla controller parameterization and to fault tolerant/detection schemes. Furthermore, the proposed framework provides a transparent analysis of the interactions between the different design parameters which allows for a clearer design trade-off between robust stability and robust performance for the saturated and unsaturated closed loops.

I. INTRODUCTION

Anti-windup (AW) compensation is a common approach used by control engineers to cope with actuator saturation, with many methods available to assist with its design (see, for example [2], [8], [18] and references therein). With few exceptions, most available methods tackle the problems of stability and performance by (implicitly) assuming that the AW design inherits the robustness properties of the robust linear system [11], [20]. This makes some intuitive sense and if the uncertainty present in the real system is sufficiently small, standard AW techniques can be applied with some confidence. On the other hand, in [17] it was argued that robust stability of the linear system was only a *necessary* condition for robust stability of the saturated closed-loop system. Indeed, in that reference an example was given of a saturated closed-loop system which behaved well using a “good” static AW design but was actually destabilized when uncertainty was introduced.

Recently, several researchers [6], [17], [5] have approached the *robust* anti-windup problem by trying to incorporate robustness directly into the design of the anti-windup compensator or by adding additional filters to improve the robustness of the nominal AW compensator.

The authors are with the Dept. of Engineering, University of Leicester, University Road, Leicester, LE1 7RH, U.K., Email: {ame12, mct6, ixp}@le.ac.uk. Corresponding author is now with Deimos Space S.L., Madrid, Spain., Email: andres.marcos@deimos-space.com

The aim of this paper is to present a general framework for robust anti-windup design and analysis. The resulting architecture provides a transparent analysis of the interactions between the different design parameters which allows for a clearer design trade-off between robust stability and robust performance for the saturated and unsaturated closed loops. It is shown that the robust AW design depends on three design parameters: two arising from the left and right coprime factors of the nominal plant, and the third the well-known free-parameter from the Youla controller parameterization. An apparent disadvantage of the proposed architecture is the increase in number of states due to the use of three design parameters (although this increase is intrinsic to similar approaches). However, in contrast to other approaches, this increase in states is offset by the possible use of the design parameters for fault tolerant control (FTC) and fault detection and isolation (FDI) objectives. It is emphasized that these connections to other areas in the control field are very useful for the analysis of interactions between different compensators and for future research.

II. ROBUST ANTI-WINDUP PROBLEM DEFINITION

A. Standard Anti-windup

Traditionally, the aim of AW compensation was rather subjective, although now [11], [20], [21] it is accepted to mean the modification of a nominal (linear) controller – with good performance and robustness in the unconstrained case – so that the following AW objectives are fulfilled:

1. The nominal closed loop performance and robustness are achieved when the initial conditions and reference signals do not cause saturation.
2. In the event of saturation, the constrained response is close to the unconstrained behaviour (although obviously limited by infeasible demands).
3. The recovery of the nominal characteristics after saturation is fast.

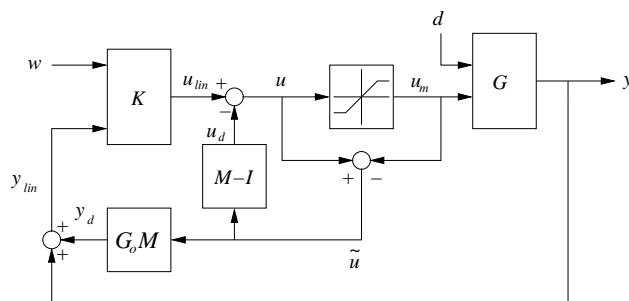


Fig. 1. Weston-Postlethwaite AW scheme.

A scheme that represents most AW configurations was proposed in [20], where the anti-windup problem is parameterized by a single transfer function, $M \in \mathcal{RH}_\infty$. Figure 1 illustrates

this AW scheme where the linear controller $K = [K_w \ K_o]$ is conditioned by the AW compensator $K_{AW} = [(M-I)' \ (G_o M)']'$. The plant $G = [G_d \ G_o] \in \mathcal{RH}_\infty$ is assumed stable in order for global stability results to be obtained. The signal $w \in \mathbb{R}^{n_w}$ is the reference command, $d \in \mathbb{R}^{n_d}$ is the plant disturbance, $y \in \mathbb{R}^p$ the plant output, the control signal is $u \in \mathbb{R}^m$ and the actual plant input is $\text{sat}(u) = u_m \in \mathbb{R}^m$. $u_d \in \mathbb{R}^m$ and $y_d \in \mathbb{R}^p$ are signals produced by the AW compensator K_{AW} .

The saturation and deadzone functions are defined as $\text{sat}(u) := [\text{sat}_1(u_1) \ \dots \ \text{sat}_m(u_m)]^T$ and $\text{Dz}(u) := [\text{Dz}_1(u_1) \ \dots \ \text{Dz}_m(u_m)]^T$ respectively, where for all $i \in \{1, \dots, m\}$ the saturation nonlinearity is given by $\text{sat}_i(u_i) := \text{sign}(u_i) \min(|u_i|, \bar{u}_i)$; the dead-zone by $\text{Dz}_i(u_i) := \text{sign}(u_i) \max(0, |u_i| - \bar{u}_i)$; and $\bar{u}_i > 0$ is a fixed bound. These functions are related by the identity $\text{sat}_i(u_i) = u_i - \text{Dz}_i(u_i)$.

The parameterization in terms of M proposed in [20] can be interpreted as the dual of that introduced in [11] which represents most linear AW schemes. However, the appeal of the former parameterization is that, using the above identity, it follows that Figure 1 can be redrawn as in Figure 2. This reveals an attractive decoupling into a nominal linear system, a nonlinear loop and a disturbance filter. If no saturation occurs ($\tilde{u} = 0$), then the nominal linear system alone determines the system's behaviour. However, if saturation occurs ($\tilde{u} \neq 0$), the nonlinear loop and disturbance filter become active. Also, note that the dynamics of the disturbance filter determine the manner in which the nominal linear behaviour is affected during and after saturation. Most interestingly, under the assumptions that the nominal linear closed-loop is asymptotically stable and $G_o \in \mathcal{RH}_\infty$, the question of global stability is thus translated into determining whether the nonlinear loop is stable.

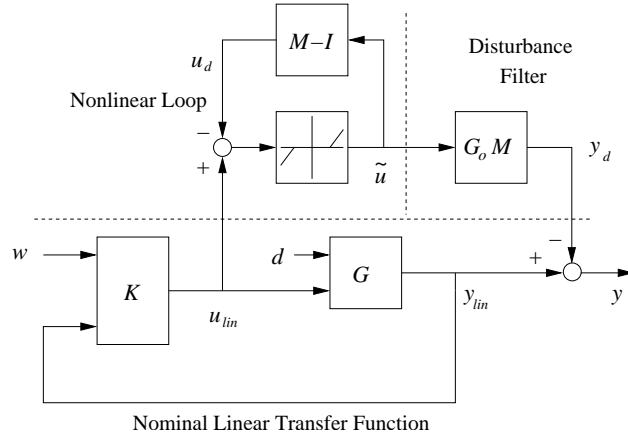


Fig. 2. W&P-AW analytical representation.

B. Anti-windup with uncertainty

As stressed in [18], most anti-windup schemes assume that the model of the plant is a good representation of the true system and do not account for uncertainty explicitly (they assume

Case 3. Uncertainty ($\tilde{r} \neq 0$), no saturation ($\tilde{u} = 0$). The filter $Q[\tilde{N}_o u_{lin} - \tilde{M}y]$ becomes a robustifying compensator $-Q\tilde{M}[\Delta_G u_{lin}]$ that can be designed to minimize the uncertainty effect on the nominal loop (G_o, K).

Case 4. Uncertainty ($\tilde{r} \neq 0$) and saturation ($\tilde{u} \neq 0$). Similarly to the previous case, the filter $Q\tilde{M}$ represents an additional degree-of-freedom to robustify the saturated closed loop.

In particular, note that key signals which dictate the operation of the scheme are \tilde{u} and \tilde{r} and that the nominal AW scheme (Case 2) and the standard high-performance control scheme (Case 3) become special cases of the above architecture. The novelty in this work is Case 4 which neither the standard (or robust) AW schemes or the high-performance control schemes address adequately: the case of uncertainty *and* saturation.

A. Analysis of the robust AW scheme

A key goal of the proposed robust AW scheme is the incorporation of the “nice” analytical nature of W&P-AW scheme. Thus, following similar algebraic manipulations used to re-draw Figure 1 as Figure 2, it is straightforward to see that Figure 4 can be re-drawn as Figure 5. Not surprisingly this new analytical scheme also boasts similar partitions to Figure 2: linear loop, nonlinear loop, and disturbance filter (now also with an additional robustification filter). This forms the basis of our subsequent analysis.

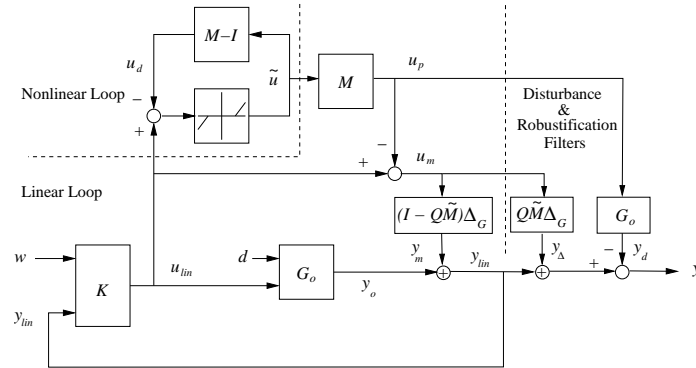


Fig. 5. Analytical representation of the robust AW architecture.

Observe from Figure 5 that the “linear” and nonlinear loops are still coupled although this time through the term $y_m = (I - Q\tilde{M})\Delta_G u_m$. Also, there is a further coupling to the outer loop $y = y_{lin} + y_\Delta - y_d$ due to the robustification filter $y_\Delta = Q\tilde{M}\Delta_G u_m$. In particular, notice that the nominal performance operator $\mathcal{T}_p(M)$ is completely independent of \tilde{M} and Q , whereas this is patently not the case for the “robustness filters” $(I - Q\tilde{M})\Delta_G$ and $Q\tilde{M}\Delta_G$. Moreover, a large

amount of design freedom lies in the free parameter, Q , and there are two particularly striking choices:

- 1) $Q = 0$. In this case the results of [17], Figure 2, are recovered; the coupling to the outer loop is lost while the coupling between the linear and nonlinear loops occurs due to the uncertainty Δ_G . This implies that nominal stability is affected by uncertainty and saturation, and therefore the design of AW compensators needs to account for this coupling. Furthermore, global stability conditions are limited by the Small-Gain Theorem – see Section II. Therefore, M must be used as before to address both performance (\mathcal{T}_p) and robustness (\mathcal{T}_r) simultaneously.
- 2) $Q = \tilde{M}^{-1}$. In this case a complete decoupling of the linear and nonlinear loops is obtained. It represents a loop shifting of the uncertainty coupling from the inner linear loop to the outer loop. This has obvious advantages as in this case a Small-Gain condition for global stability of the saturated system is *not necessary* (although it is desirable for robust performance). Moreover, this implies that minimization of the map $\mathcal{T}_p : u_{lin} \mapsto y_d$ (as in [18]) would automatically result in a stable system, regardless of the uncertainty present. In particular note that M now need only address the performance operator, \mathcal{T}_p .

Therefore, choosing $Q = \tilde{M}^{-1}$ essentially implies *unconditional robust stability* at the expense of *robust performance*; while $Q = 0$, implies the potential of nominal robustness recovery during saturation and nominal linear behaviour in the absence of saturation. Furthermore, the above analysis together with the clear presentation in Figure 5 of the uncertainty effect on *robust stability* and *robust performance*, allows the analysis and trade-off of these conflicting objectives (through the parameter Q) by using the operators $\mathcal{T}_{RS} : u_{lin} \rightarrow y_m$ and $\mathcal{T}_{RP} : u_{lin} \rightarrow y_\Delta$. Note that this is in contrast to the conventional robust AW problem where the trade-off is between *robust stability* and *nominal performance*. In the generalized robust AW problem, the nominal performance problem is unaffected.

IV. SYNTHESIS OF THE DESIGN PARAMETERS

The analysis above essentially provides three free parameters to the designer for robust AW design: M , \tilde{M} and Q . As the nominal performance map $\mathcal{T}_p(M) : u_{lin} \rightarrow y_d$ is *independent* of both \tilde{M} and Q it is suggested that M is thus chosen to satisfy nominal (un-perturbed) AW stability and performance objectives, i.e. to ensure the nonlinear loop is stable and $\|\mathcal{T}_p(M)\|_{i,2}$ is minimized. It therefore remains to choose \tilde{M} and Q to trade-off robust stability and robust performance objectives once M has been chosen to capture nominal AW objectives, i.e. minimizing $\mathcal{T}_{RS} : u_{lin} \rightarrow y_m$ versus minimizing $\mathcal{T}_{RP} : u_{lin} \rightarrow y_\Delta$. Additionally, from Figure 4, the factors \tilde{N}_o and \tilde{M} can be designed so that the primary residual signal \tilde{r} better captures the uncertainty.

These design tasks can be simplified using coprime factorizations of the plant. Following [20], M can be chosen as part of a coprime factorization of the nominal plant $G_o = NM^{-1}$. Similarly,

following [1], [23], \tilde{M} can be chosen as left coprime factorization of the nominal plant $G_o = \tilde{M}^{-1}\tilde{N}$. Therefore, assigning to the plant the minimal state-space realization $G_o \sim (A, B, C, D)$, suitable plant-order coprime factorizations can be chosen as

$$\begin{bmatrix} M-I \\ N_o \end{bmatrix} = \left[\begin{array}{c|c} A+BF & B \\ \hline F & 0 \\ C+DF & D \end{array} \right] \quad (1)$$

$$\begin{bmatrix} \tilde{N}_o & \tilde{M} \end{bmatrix} = \left[\begin{array}{c|cc} A+LC & B+LD & L \\ \hline C & D & I \end{array} \right] \quad (2)$$

where F and L are the state feedback and observer gains chosen so that $(A+BF)$ and $(A+LC)$ are stable and the AW requirements [17] (and if desired residual generation objectives [3]) are satisfied.

The design of the parameter Q will be constrained by the need to trade-off between robust stability and robust performance for the saturated and unsaturated cases. From Figure 5, and as mentioned above, the two key robust stability and robust performance mappings are $\mathcal{T}_{RS} : u_{lin} \rightarrow y_m$ and $\mathcal{T}_{RP} : u_{lin} \rightarrow y_\Delta$. Thus, the design of Q can be sensibly posed as finding:

$$\mu := \min_{Q(s), \tilde{M}(s) \in \mathcal{RH}_\infty} \left\| \left[\begin{array}{c} W_1 \mathcal{T}_{RS} \\ W_2 \mathcal{T}_{RP} \end{array} \right] \right\|_{i,2} \quad (3)$$

where W_1 and W_2 are linear operators associated with some appropriate transfer function matrices¹.

This is a difficult optimization problem; however, note that:

$$\begin{aligned} \mu &= \min_{Q(s), \tilde{M}(s) \in \mathcal{RH}_\infty} \left\| \left[\begin{array}{c} W_1(I-Q\tilde{M}) \\ W_2Q\tilde{M} \end{array} \right] \Delta_G \mathcal{T}_r \right\|_{i,2} \leq \min_{Q(s), \tilde{M}(s) \in \mathcal{RH}_\infty} \left(\left\| \left[\begin{array}{c} W_1(I-Q\tilde{M}) \\ W_2Q\tilde{M} \end{array} \right] \right\|_{i,\infty} \|\Delta_G\|_\infty \|\mathcal{T}_r\|_{i,2} \right) \\ &= \|\Delta_G\|_\infty \|\mathcal{T}_r\|_{i,2} \underbrace{\min_{Q(s), \tilde{M}(s) \in \mathcal{RH}_\infty} \left\| \left[\begin{array}{c} W_1(I-Q\tilde{M}) \\ W_2Q\tilde{M} \end{array} \right] \right\|_{i,\infty}}_{\gamma_{RS/RP}} \end{aligned} \quad (4)$$

So the optimization in equation (3) reduces to the standard \mathcal{H}_∞ optimization problem:

$$\gamma_{RS/RP} = \min_{Q(s), \tilde{M}(s) \in \mathcal{RH}_\infty} \left\| \left[\begin{array}{c} W_1(I-Q\tilde{M}) \\ W_2Q\tilde{M} \end{array} \right] \right\|_{i,\infty} \quad (5)$$

Thus, the following algorithm is proposed for the design of high-performance robust AW compensators:

¹We do not distinguish between a rational linear operator and its transfer function.

- Step 1. Design a high-performance 2 Degree-of-Freedom (DoF) controller $K = [K_w \ K_o]$ (i.e. satisfying performance/stability for the *nominal* plant G_o under no saturation).
- Step 2. Design a nominal AW compensator, i.e. design $M \equiv$ design F in equation (1) [20], to satisfy nominal anti-windup objectives: i) minimization of the deviation between the behaviour of the nonlinear and linear loops during saturation, and ii) fast recovery of the linear behaviour after saturation.
- Step 3. Design the coprime factors \tilde{M} and \tilde{N}_o , i.e. find L in equation (2) [3], so that the primary residual \tilde{r} provides a measure of the presence of uncertainty (e.g. in a H_∞ setting it might be the maximum norm difference with respect to G_o).
- Step 4. Design Q using equation (5) so that the nominal performance objectives achieved in steps 1 and 2 are minimally degraded in the presence of uncertainty.

Although only plant uncertainty has been assumed, steps 3 and 4 in the above algorithm can also be used to robustify the closed loop against performance loss due to exogenous disturbances. Indeed, the proposed robust AW framework is also suitable for fault tolerant control (FTC) design and/or fault detection and isolation (FDI) purposes, see Section VI.

V. LOW-ORDER DESIGN AND IMPLEMENTATION OF THE ROBUST AW ARCHITECTURE

The proposed robust AW scheme, as implemented in Figure 4, will increase the total number of states in the closed loop by n_q plus $5n_p$ states in addition to the states of the nominal controller K , and the actuator and sensor dynamics. This increase in states comes from the independent blocks used for the AW compensator, namely $(M-I)$ and G_oM which add a total of $3n_p$ states, and the robustifying compensator, Q , \tilde{N}_o and \tilde{M} which add the remaining $2n_p + n_q$. Although this implementation structure is attractive for presentation and analysis purposes, it is not satisfactory for practical implementation in systems such as those found in the aerospace [16] and hard-disk fields [9] where the computational power available is limited.

In practice, the implementation will use the connection of the proposed robust AW scheme with the Youla parameterization² to reduce the number of states. Indeed, following the standard implementation of the coprime factors as given in equations (1) and (2), the final number of states required by the robust AW scheme is $2n_p + n_q$, see Figure 6.

It is clear from Figure 6 that there are three main sub-systems where further reduction in the number of states can be achieved for the overall robust AW compensator: the residual generator factors $[\tilde{N}_o \ \tilde{M}]$, the robustifying parameter Q , and the standard AW compensator $[M' - I \ N_o]'$.

In order to reduce the order of the residual generator factors \tilde{N}_o and \tilde{M} , an initial reduced model of the plant \hat{G}_o , from which these factors are synthesized, could be obtained or they could be reduced using the frequency-weighted coprime factor reduction approach from [19].

²This is interesting in its own right, but space prevents a full discussion of this

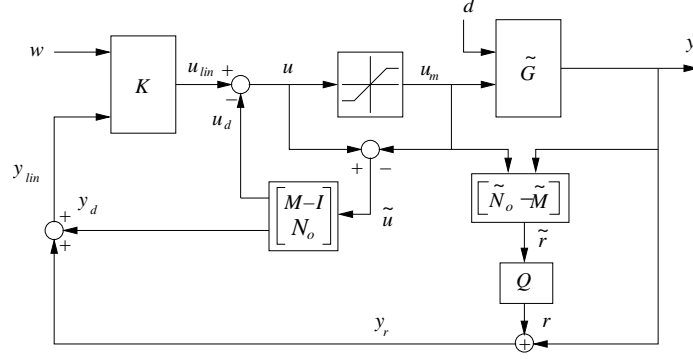


Fig. 6. Practical implementation of the robust AW architecture.

In terms of reducing the state dimension of Q , a possible approach can be based on the global stability requirement that the plant \tilde{G} is exponentially stable³. In this case, the implementation of the residual generator could be given by $\tilde{r} = Q(G_o u_m - y)$, i.e. $\tilde{N}_o = G_o$ and $\tilde{M} = I$. Using this special factorization, the \mathcal{H}_∞ -optimization used in step 3 of the synthesis algorithm, equation (5), can be transformed to that of seeking:

$$Q^*(s) = \arg \min_{Q(s) \in \mathcal{RH}_\infty} \left\| \begin{bmatrix} W_1(I-Q) \\ W_2Q \end{bmatrix} \right\|_\infty \quad (6)$$

which results in a lower-order Q since the coprime factor \tilde{M} does not introduce additional states.

Furthermore, in \mathcal{H}_∞ -optimization, the weights W_1, W_2 are typically chosen to be of low-order so that the resulting state dimension for Q can be further reduced. In the special case that the weights can be chosen real and static, and using the special global stability coprime factorization, Q can be chosen real and static and the previous \mathcal{H}_∞ optimization procedure can be replaced with something simpler which will yield a static robustifying Q parameter.

In order to do this, define $W_0 := [W_1' \ 0]'$ and the full column rank matrix $\bar{W} := [-W_1' \ W_2']'$ with $\bar{W}'\bar{W} = \Phi$, where Φ is a full rank real matrix. Also, let \bar{W}_\perp be a matrix with columns which span the null space of \bar{W}' . Then $\bar{W}_\perp'\bar{W} = 0$ and $[\bar{W} \ \bar{W}_\perp]$ is full rank. Furthermore, there exists a choice of \bar{W}_\perp such that $\Phi^{-\frac{1}{2}}[\bar{W} \ \bar{W}_\perp]$ is an orthogonal matrix. From this we have that:

$$Q^* = \min_Q \left\| \begin{bmatrix} W_1(I-Q) \\ W_2Q \end{bmatrix} \right\| = \min_Q \|\Phi^{-\frac{1}{2}}[\bar{W} \ \bar{W}_\perp]'(W_0 + \bar{W}Q)\| \quad (7)$$

It then follows from Parrot's Theorem (see Section 2.11 of [22]) that Q^* can be computed from:

$$\Phi^{-\frac{1}{2}}(\bar{W}'W_0 + \bar{W}'\bar{W}Q) = 0 \quad (8)$$

³This is a standard and necessary requirement for even the non-robust anti-windup problem.

with the optimal “cost” given as $\|\Phi^{-\frac{1}{2}}\bar{W}'_1 W_0\|$.

Obviously this is computationally more efficient than solving an \mathcal{H}_∞ optimization problem, although stipulating that Q is static is restrictive. More appealing solutions may be found by allowing Q to be dynamic. Moreover, low-order weights might not be possible or, as it will be seen in the following section, the globally stable factorization might not be desirable for FDI/FTC purposes. In this case, the reduction approach proposed in [23] can be used:

$$\min_{\hat{Q} \in \mathcal{RH}_\infty} \left\| Q[\tilde{N}_o \ \tilde{M}] - \hat{Q} \right\|_\infty \quad (9)$$

where \hat{Q} is restricted to a lower order transfer function.

The proposed approach is particularly useful for static or low order AW compensation approaches [18] where the AW compensator is designed such that it contains either no states, or a number less than the order of the plant. Static AW compensation is particularly appealing due to its simplicity and ease of implementation (by definition it adds no extra states) and low order compensators have similar appeal. In the static case, the dynamic AW compensator from Figure 6, $[u'_d \ y'_d]' = [(M-1)' \ N'_o]'$, is substituted by $\Theta = [\Theta_1' \ \Theta_2']'$ which emits two signals $\theta_1 \in \mathbb{R}^m$ and $\theta_2 \in \mathbb{R}^p$ equivalent to u_d and y_d . More generality of the scheme can be obtained by injecting θ_2 directly into the controller state equation, as suggested in [7], [10], instead of at the controller input although this may not always be possible in practical problems. However, these more general results can be recovered in the framework adopted here by appropriately augmenting the controller input distribution matrix with extra columns and the output y with extra null entries [14]. In this case our overall AW compensator, K_{AW} will have order $n_p + n_Q$, which is not much higher than standard robust AW [17].

VI. CONNECTION TO FAULT DETECTION AND FAULT TOLERANT SCHEMES

One of the main advantages of the proposed architecture is its connection to the fields of fault detection & isolation (FDI) and fault tolerant control (FTC) through the well-known residual generator concept given by $\hat{r} = \tilde{N}_o u_m - \tilde{M}y$ in Figure 4, see references [3], [1], [13], [12]. As mentioned above the presence of extra states in the residual generator $[\tilde{N}_o \ \tilde{M}]$ may be acceptable as they can be harnessed for FDI and FTC purposes. This represents also quite a novel line of research as to the best of our knowledge no published paper has dealt with the intersection of input saturation and fault effects (and the architecture proposed in this paper is ideally suitable to analyze this important topic).

Figure 7 shows the breakdown of the proposed robust AW architecture elements in terms of their primary objective: nominal anti-windup, residual generation and FDI/FTC capabilities.

For FDI purposes, a filter Q_f is added to the primary residual \tilde{r} and chosen to minimize the effects of uncertainty Δ_G and disturbances d while maximizing those from sensor f_{sen} and

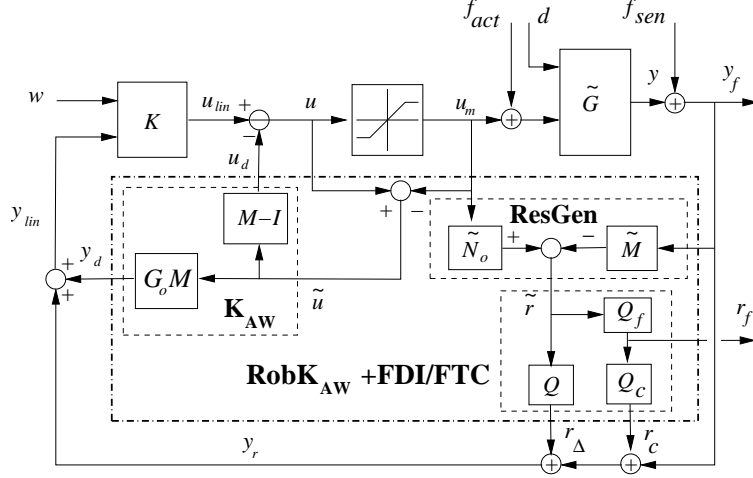


Fig. 7. General Robust AW architecture with FDI/FTC capability.

actuator f_{act} faults (to facilitate presentation, it is assumed that $\Delta_G = d = 0$ in equation (10)):

$$r_f = Q_f (\tilde{N}_o u_m - \tilde{M} y_f) = Q_f (\tilde{N}_o u_m - \tilde{M} (f_{sen} + G_o u_m + G_o f_{act})) = -Q_f (\tilde{M} f_{sen} + \tilde{N}_o f_{act}) \quad (10)$$

Note that the fault residual signal r_f is not typically fed back to the controller unless required for fault tolerant control purposes [1], [13]. In the latter case, a fault tolerant parameter Q_c (with similar role to Q in the proposed robust AW architecture) that uses the fault residual signal is added to the feedback signal to the controller, i.e. $y_r = y_f + r_\Delta + r_c$ where $r_c = Q_c r_f$. Thus the proposed approach is attractive because it provides an architecture for robust AW, and FDI and FTC.

VII. MASS-SPRING-DAMPER EXAMPLE

The nominal and perturbed mass-spring-damper example from references [21], [17] is used to demonstrate the robust AW approach. The state-space of the nominal plant G_o is given by:

$$A_o = \begin{bmatrix} 0 & 1 \\ -10 & -10 \end{bmatrix}; B_o = \begin{bmatrix} 0 \\ 10 \end{bmatrix}; C_o = [1 \ 0]; D_o = [0]; \quad (11)$$

A two-degrees-of-freedom linear controller with acceptable performance (fast convergent response, no steady-state error, no overshoot) and robustness (asymptotic tracking and rejection of step disturbances) is given in the same two references. Its state-space is $K = [K_w \ K_o] \sim$

$(A_c, [B_{cr} \ B_c], C_c, [D_{cr} \ D_c])$ where:

$$A_c = \begin{bmatrix} -80 & 0 & 2.5 \\ 1 & 0 & 0 \\ 0 & 0 & -2.5 \end{bmatrix}; B_{cr} = \begin{bmatrix} 0 \\ 0 \\ 1 \end{bmatrix}; B_c = \begin{bmatrix} -1 \\ 0 \\ 0 \end{bmatrix};$$

$$C_c = [-9450 \ 3375 \ 337.5]; D_{cr} = [0]; D_{cy} = [-135];$$

In order to highlight the possibility of acceptable low-order practical implementations (as given in Section V) and the robustification capabilities of the proposed approach, the quadratically stabilizable static anti-windup compensator given in [17] is used⁴, $\Theta = [-0.1909 \ 0.1402]^\top$. Therefore, the low-order implementation from Figure 6 is used with the AW compensator $[(M - I)' \ N_o']'$ substituted by the static gains from Θ , and the normalized left coprime factors of the nominal plant, \tilde{N}_o and \tilde{M} , obtained using standard factorization techniques [4].

First, the nominal plant output responses (with $Q = 0$) are shown in Figure 8. The thick solid and dashed-dot lines are the responses of the nominal, and with no AW, closed-loop system under the unconstrained and the constrained (plant input saturation limited to ± 1 meters) environments, respectively. It is observed that for the input saturation case, the response has degraded and it is out-of-phase with respect to the unsaturated response. The thick dashed line in the figure shows the response of the nominal saturated closed loop with the static AW compensator. It shows performance improvement since the response is now in-phase with the reference command (although the infeasibility of the command prevents correct steady-state tracking beyond the saturation magnitude).

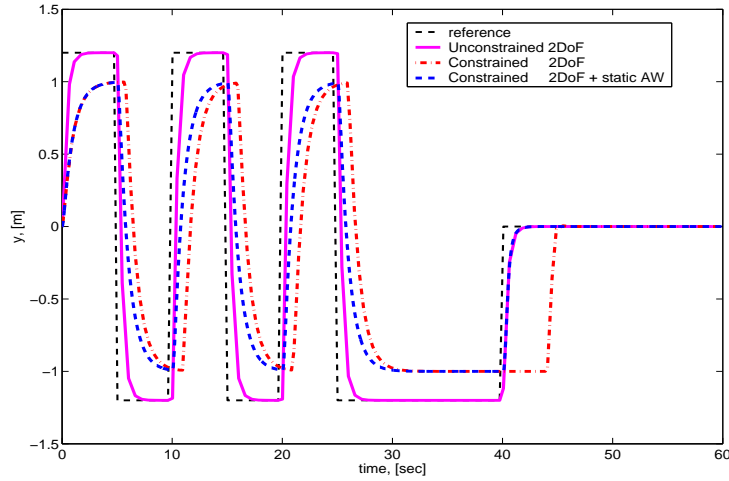


Fig. 8. Responses of the nominal closed loops with $Q = 0$.

⁴It is known that this static AW design is not stable for the saturated perturbed system (shown later).

Next, we examine the case of the true, or perturbed, plant $\tilde{G} = G_o + \Delta_G$ which has a large resonant peak. Its state-space representation is given by:

$$A_p = \begin{bmatrix} 0 & 1 \\ -10 & -0.01 \end{bmatrix}; B_p = B_o; C_p = C_o; D_p = D_o; \quad (12)$$

Note that the true plant in equation (12) implies a large perturbation away from the nominal plant in equation (11): the open-loop poles change from $(-8.87, -1.13)$ to $-0.05 \pm 3.16j$. Figure 9 shows the same responses as before but now using the perturbed plant. It is noted that the perturbed response of the constrained linear 2 DoF controller without AW (the thick dashed-dot line) is robust to the uncertainty and only results in an oscillatory behaviour during transients in comparison to its nominal response from Figure 8 (it still contains the out-of-phase characteristic). On the other hand, it is clear that the static AW (thin dashed line) not only did not inherit the robustness properties of the linear closed loop but it has also become unstable.

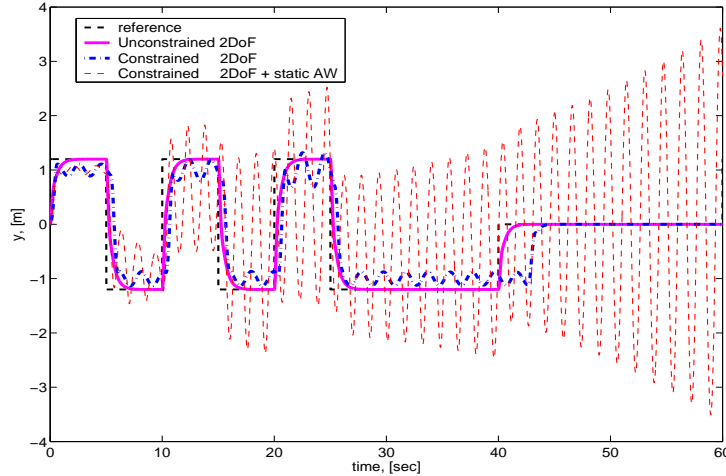


Fig. 9. Responses of the perturbed closed loops with $Q = 0$.

Using the proposed robust AW approach and the optimization set-up from equation (5), three robustifying compensators are obtained to address the lack of robustness for the saturated closed loop with the static AW. The optimization weights W_1 and W_2 are set to constants to keep the number of states to a minimum (since no order-reduction on \tilde{M} is performed, and $\tilde{M} \neq I$, the number of states is two for all the Q filters). Table I shows the selected weights for the three robustifying filters (together with the H_∞ -norms of the scaled RS and RP transfer functions – the less the norm the better). Q_{des} is optimized to provide a good compromise between robust stability (RS) and robust performance (RP). The subsequent filters are designed focusing more on the robust stability Q_{RS} or the robust performance Q_{RP} . Since the primary residual signal \tilde{r} is identically to zero when no uncertainty is considered in the system, the time responses for

TABLE I
ROBUSTIFYING FILTERS.

	W_1	W_2	RP= $\ Q\tilde{M}\ _\infty$	RS= $\ (I-Q\tilde{M})\ _\infty$
Q_{des}	1	2.5	0.1379	0.8621
Q_{RS}	5	1	0.9615	0.0385
Q_{RP}	1	5	0.0385	0.9615

the nominal plant are exactly those given in Figure 8 for the three robustifying filters. For the case of the perturbed system and Q_{des} , designed to trade-off RS and RP, the output responses for the unsaturated and saturated closed loops are shown in Figure 10.

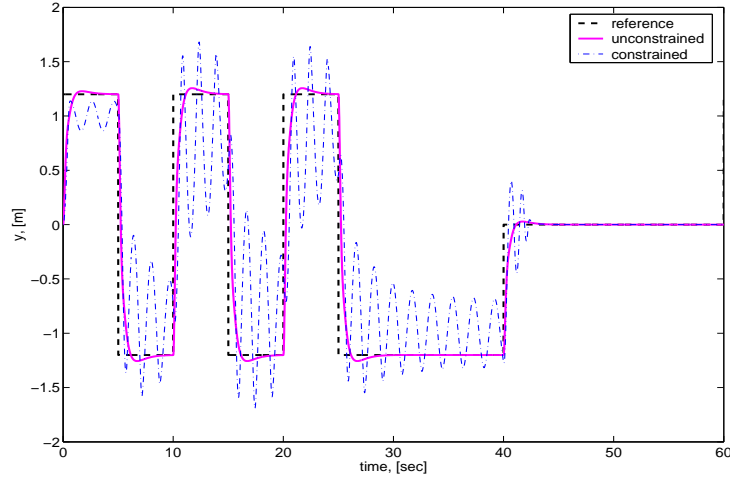


Fig. 10. Output y of the robustified static AW perturbed closed loops (Q_{des}).

Observe that there is a slight loss of performance (i.e. small overshoot) for the unconstrained response (thick solid line) arising from the contribution of the filtered uncertainty. For the saturated case (thin dashed-dot line), it is clear that the new scheme has succeeded in robustifying the static anti-windup since the response is now stable, albeit oscillatory during saturation.

Finally, the output y and linear output y_{lin} responses – Figures 11 and 12 respectively – for the perturbed, saturated closed loops are presented for the two other robustifying filters, Q_{RS} and Q_{RP} . Figure 11 shows that when the weight for the robust performance W_2 is more heavily penalized the resulting filter Q_{RP} is better, i.e. the oscillation is smaller and the convergence to the steady-state faster than with the filter obtained with a higher penalty on the robust stability weight W_1 (which is still better than $Q = 0$ but highly oscillatory during saturation).

Figure 12 shows the time responses for the linear output, i.e. the input y_{lin} to the controller which is the signal used for robust stability – see the analytical diagram in Figure 5. As expected

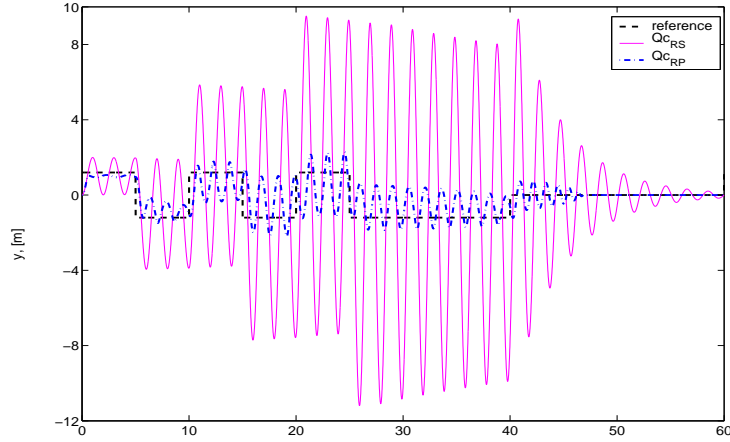


Fig. 11. Output y of the robustified static AW perturbed closed loops (Q_{RS} and Q_{RP}).

the filter designed for robust stability Q_{RS} is now better than that for robust performance. Note as well, that the small oscillation with Q_{RS} is endemic to the controller K and unavoidable unless the controller is redesigned. To see this, compare the response to the constrained response for the perturbed closed loop with no robustifying filter from Figure 9.

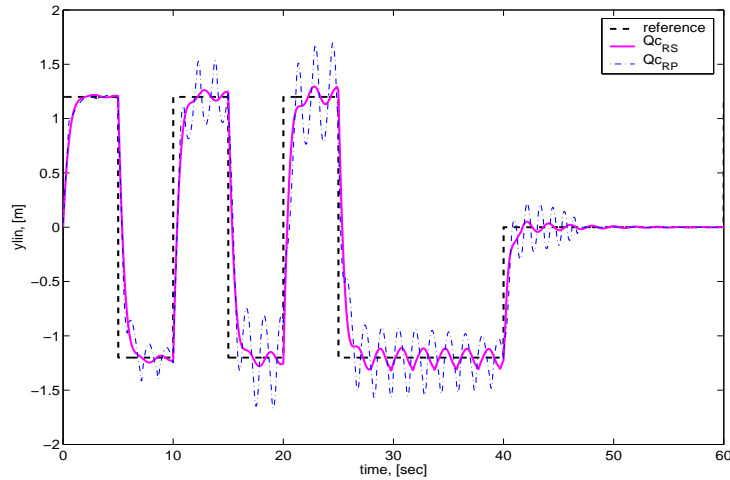


Fig. 12. Linear output y_{lin} of the robustified static AW perturbed closed loops (Q_{RS} and Q_{RP}).

VIII. CONCLUSIONS

A general framework for the design and analysis of high-performance robust anti-windup compensators has been presented for stable plants (stable due to global stability requirements).

The proposed framework combines the W&P-AW scheme with a high-performance control architecture which includes a residual generator. This combination of schemes provides an analytical framework where the interactions between the different design parameters are transparent and can be used to simplify the trade-off between robust stability and robust performance in the saturated and unsaturated cases. Furthermore, it has been shown that the framework is closely connected to FDI/FTC schemes. A simple mass-spring-damper system has been used to exemplify the design of robustifying filters for a static AW scheme which made the saturated closed loop unstable in the presence of uncertainty.

Finally, it is important to remark that the scheme proposed here is closely related to the “weakened” AW approach of [5] and in some senses generalizes that work. In fact, tedious algebra shows that the parameter F_{rob} used in that work is actually equivalent to $F_{rob} = I - Q$ in the proposed framework. The work here thus gives [5] an appealing graphical interpretation and shows how it is connected with the wider control literature.

REFERENCES

- [1] Chen, J. and Patton, R.J. *Robust Model-Based Fault Diagnosis for Dynamic Systems*. Kluwer Academic Publishers, 1999.
- [2] Crawshaw, S. and Vinnicombe, G. Anti-windup synthesis for guaranteed L_2 performance. In *IEEE Conference on Decision and Control*, Sydney, Australia, December 2000.
- [3] Ding, X. and Frank, P.M. Fault Detection via Factorization Approach. *Systems and Control Letters*, 14:431–436, 1990.
- [4] Francis, B.A. *A course in \mathcal{H}_∞ Control Theory*, volume 88 of *Lecture Notes in Control and Information Sciences*. Springer-Verlag, 1986.
- [5] Galeani, S., Nicosia, S., Teel, A.R., and Zaccarian, L. Output feedback compensators for weakened anti-windup of additively perturbed systems. In *IFAC World Congress*, Prague, July 2005.
- [6] Garcia, G., Tarbouriech, S., Suarez, R., and Alvarez-Ramirez, J. Nonlinear bounded control for norm-bounded uncertain systems. *IEEE Transactions on Automatic Control*, 44(8):1254–1258, 1999.
- [7] Grimm, G., Hatfield, J., Postlethwaite, I., Teel, A.R., Turner, M.C., and Zaccarian, L. Anti-windup for stable linear systems with input saturation: an LMI based synthesis. *IEEE Transactions on Automatic Control*, 48(9):1509–1525, 2003.
- [8] Hanus, R., Kinnaert, M., and Henrotte, J.L. Conditioning technique, a general anti-windup and bumpless transfer method. *Automatica*, 23(6):729–739, 1987.
- [9] Herrmann, G.H., Turner, M.C., and Postlethwaite, I. Practical implementation of a novel anti-windup scheme in a HDD dual stage servo system. *IEEE/ASME Transactions on Mechatronics*, 9(3):580–592, 2004.
- [10] Kapoor, N., Teel, A.R., and Daoutidis, P. An anti-windup design for linear systems with input saturation. *Automatica*, 34(5):559–574, 1998.
- [11] Kothare, M.V., Campo, P.J., Morari, M., and Nett, C.N. A unified framework for the study of anti-windup designs. *Automatica*, 30(12):1869–1883, 1994.
- [12] Marcos, A. and Balas, G.J. A robust integrated controller/diagnosis aircraft application. *International Journal of Robust and Nonlinear Control*, 15(12):531–551, 2005.
- [13] Marcos, A., Ganguli, S., and Balas, G.J. New Strategies for Fault Tolerant Control and Fault Diagnostic. In *5th IFAC Symposium on Fault Detection, Supervision and Safety of Technical Processes*, Washington, D.C, June 2003.
- [14] Marcos, A., Turner, M.C., Bates, D.G., and Postlethwaite, I. Robustification of static and low order anti-windup designs. In *5th IFAC Symposium on Robust Control Design, ROCOND*, Toulouse, FR, July 2006.
- [15] Tay, T.T., Mareels, I., and Moore, J.B. *High Performance Control*. Birkhauser, 1998.
- [16] Turner, M.C., Walker, D.J., and Alford, A.G. Design and Ground-based Simulation of an \mathcal{H}_∞ Limited Authority Flight Control System for the Westland Lynx Helicopter. *Aerospace Science and Technology*, 5(3):221–234.

- [17] Turner, M.C., Herrmann, G., and Postlethwaite, I. Accounting for uncertainty in anti-windup synthesis. In *American Control Conference*, Boston, MA, June 2004.
- [18] Turner, M.C. and Postlethwaite, I. A new perspective on static and low order anti-windup synthesis. *International Journal of Control*, 77(1):27–44, 2004.
- [19] Varga, A. On frequency-weighted coprime factorization based controller reduction. In *American Control Conference*, Denver, USA, June 2003.
- [20] Weston, P.F. and Postlethwaite, I. Linear conditioning for systems containing saturating actuators. *Automatica*, 36(8):1347–1354, August 2000.
- [21] Zaccarian, L. and Teel, A. A common framework for anti-windup bumpless transfer and reliable design. *Automatica*, 38(10):1735–1744, October 2002.
- [22] Zhou, K., Doyle, J.C., and Glover, K. *Robust and Optimal Control*. Prentice-Hall, Englewood Cliffs, NJ, 1996.
- [23] Zhou, K. and Ren, Z. A New Controller Architecture for High Performance, Robust, and Fault-Tolerant Control. *IEEE Transactions on Automatic Control*, 46(10):1613–1618, 2001.